Supplemental Material

Supplemental Data

In vacuum structural model of E295A

In the WT model, the turret Glu295 forms a –COO•••HN– hydrogen bond with the backbone amide of Val319 (2.79 Å) as well as van der Waals interactions with the side chain of Lys318. The latter two amino acids belong to the outer vestibule of the pore. As such, the loss of this bond network in a model of mutant E295A leads to a slight movement of the main and side chains of Val319 (Supplemental Fig. 4*A*). In the mutant model, Val319 forms van der Waals interactions with Trp304 and Asp317 of the neighboring subunit. Since Val319 interacts with Tyr315 (van der Waals) of the neighboring subunit, they both dislocate and thereby cause backbone torsion at position 315. Consequently, the carbonyl group of Tyr315 moves closer to the axis of ion conduction and the center-to-center distance between facing carbonyl oxygens becomes smaller than in the WT (5.06 Å versus 5.78 Å).

In vacuum structural model of D317A

Elimination of the bond network of D317 due to its replacement by alanine leads to movements of the backbone in the outer vestibule. The consequent torsional effects propagate to Tyr315 and eventually constrict the selectivity filter at this position to a diameter of 5.01 Å (Supplemental Fig. 4*B*).

In vacuum structural model of V310G

The WT KCNQ1 model shows that Val310 is sandwiched between Phe332 and Phe340 and also interacts with Ala336, which closes the ‘nest’ of Val310 at its back (Supplemental Fig. 4*C*). These three residues belong to S6 of the same subunit. Of particular importance, replacement of Val310 by Gly eliminates the interactions of this position with Phe332. The latter has multiple intrasubunit interactions with the backbone atoms of Gly306 and Thr309 and with the side chains of Thr309 and Trp305 (Supplemental Fig. 4*D*). Consequently, Phe332 moves closer to positions 306 and 309. This change leads to dislocation of Gly306 and Thr309 (including their backbone atoms) towards Tyr315 and Ile313. As Thr309 has multiple van der Waals interactions with Tyr315 and Ile313, the latter two slightly move and cause torsion in the backbone of the selectivity filter. Again, the effect is observed at position 315 of the selectivity filter, where the distance between the carbonyl oxygens across the pore becomes smaller (5.15Å versus 5.78Å).

Supplemental Figure Legends

Supplemental Figure 1. Coexpression of KCNE1 with WT KCNQ1 and mutant L273F in CHO cells. *A*, Representative traces of WT KCNQ1 coexpressed with KCNE1. Held at -90 mV, CHO cells were stepped for 3 sec from -60 mV to +60 mV in 10 mV increments and repolarized at -60 mV. *B*, Representative traces of L273F coexpressed with KCNE1. Currents were evoked as in *A*. *C*, Current density-voltage relations of WT KCNQ1+KCNE1 (solid circles) and L273F+KCNE1 (empty circles) (n = 6).

Supplemental Figure 2. Kinetic parameters of Ba^{2+} block in WT, L273F and L273W. *A*, Slow (empty bars) and fast (black bars) time constants of Ba^{2+} block measured at 0 mV in WT, L273F and L273W channels, with *B*, their respective slow (empty bars) and fast (black bars) amplitude components. Data shown are means ± SEM (n = 6-8; * $p < 0.01$).

Supplemental Figure 3. Multiple sequence alignment of three K^+ channels. Shown are human KCNQ1 (Swiss-Prot P51787), rat Kv1.2 (PDB ID 2A79, chain B) and *Streptomyces lividans* KcsA (PDB ID 1BL8). Alignment was performed with the program T-COFFEE (see Methods). Black background indicates identical amino acids. Grey background indicates similarities according to size, hydrophobicity, aromaticity, charge and polarity. The identity between the aligned amino acids of KCNQ1 and Kv1.2 is 37%. The letter "h" denotes alpha helix in the 3-D structural models of WT KCNQ1 and its mutants, while amino acids of the helices' ends are located at the borderline between helical and loop structures.

Supplemental Figure 4. Structural models of mutants E295A, D317A and V310G. *A*, Superposition of mutant E295A (green) on the WT KCNQ1 (CPK) with part of the rare subunit shown in thin Cα trace (magenta). Dotted black lines correspond to distances of 2.6-2.9 Å (hydrogen bonding between E295 and V319). Dotted grey lines correspond to distances of ~3.7 Å (van der Waals interactions). *B*, Superposition of the structural models of WT KCNQ1 and mutant D317A, as in *A*. The dotted black lines reflect a distance of ~2.9 Å (hydrogen bonding). The dotted grey lines reflect a distance of 3.4-3.8 Å (polar interactions between R293 and the carbonyls of G316 and D317; van der Waals interactions between

W304 and Y315). *C*, Model of one subunit of WT KCNQ1 showing a space-filling representation of the hydrophobic residues that surround V310. The backbone carbon, nitrogen and oxygen atoms of the indicated amino acids are shown in light grey, blue and red colors respectively. *D*, Superimposition of the structural models of WT KCNQ1 and mutant V310G. The frontal subunit was removed for clarity and the models were tilted towards the viewer by ~30 degrees in order to allow better viewing of the amino acid movements that are described in the Supplemental data. The WT is shown in CPK colors (as in *A*) while, in case of the mutant, the two facing subunits are shown in green and the rare subunit is depicted in magenta. The dotted black line corresponds to a distance of ~2.7 Å (hydrogen bonding between the hydroxyl group of Y315 and Nε of W305 of the neighboring subunit). The dotted grey lines correspond to distances of 3.1-3.8 Å (van der Waals interactions). For clarity, not all plausible van der Waals interactions are shown.

Supplemental Figure 5. Mutations in the voltage sensor S4 producing voltage-dependent slow inactivation. *A* and *B*, Representative current traces of WT and L233W and Q244W, respectively, measured in transfected CHO cells. From a holding potential of -90 mV, the membrane was stepped for 3 s from -70 mV to +60 mV in 10 mV increments and then repolarized for 1.5 s to -60 mV to generate the tail currents. *C*, Percent of slow inactivation of WT, Q244W and L233W (n = 7-20) as measured by the ratio between the sustained and the peak current amplitudes.

Supplemental Table 1: Rate constant values obtained from the fit of traces recorded from mutant L273F upon step depolarizations (3 s) at +20 mV and at -60 mV.

Rate constant (s^{-1})	V = +20 mV n = 9	V = -60 mV n = 9
k_1	476.92 ± 39.57	55.94 ± 4.25
k_{-1}	5.700 ± 1.195	49.01 ± 0.26
k_2	16.18 ± 1.00	0.880 ± 0.066
k_{-2}	1.15 ± 0.42	1.504 ± 0.104
k_3	0.230 ± 0.049	0.0041 ± 0.0001
k_{-3}	0.0036 ± 0.0006	0.357 ± 0.015
k_4	43 ± 3	43 ± 3
k_{-4}	23.94 ± 1.81	23.94 ± 1.81
k_5	0.532 ± 0.110	0.030 ± 0.007
k_{-5}	1.274 ± 0.230	27.22 ± 0.44

Suppl Fig 1

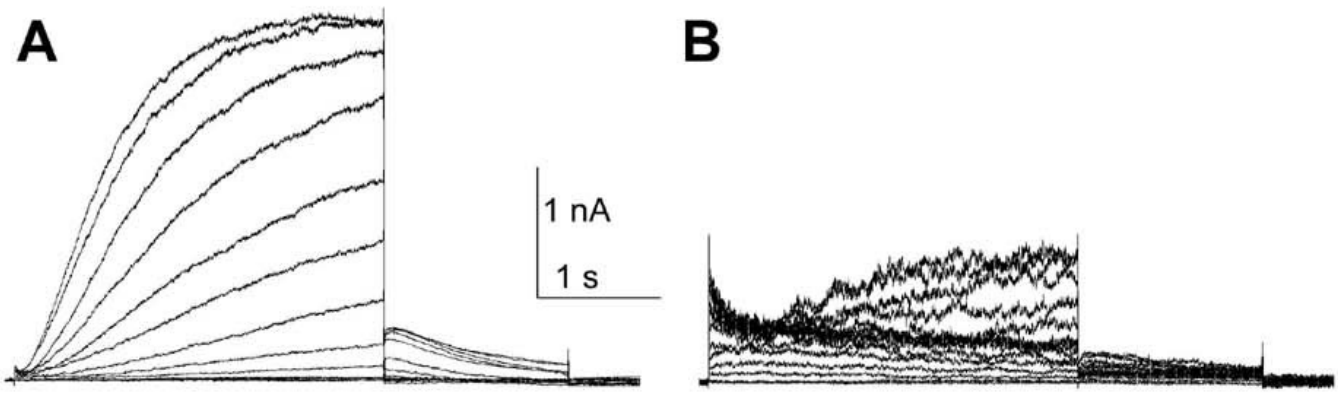
A
1 nA
1 s
B

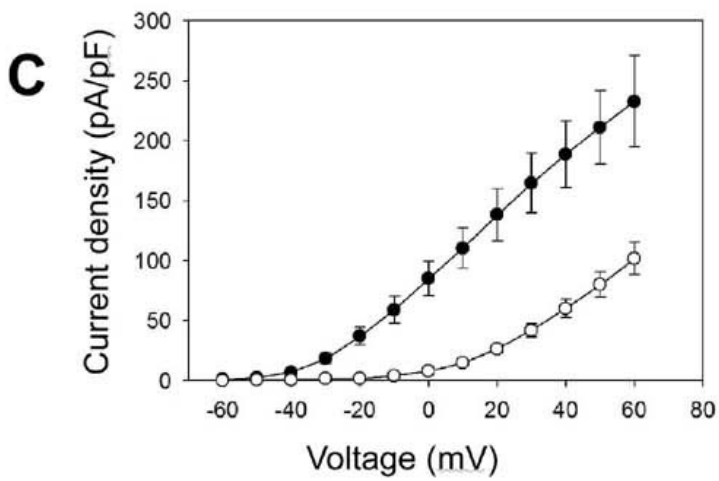
C
Current density (pA/pF)
300
250
200
150
100
50
0
-60
-40
-20
0
20
40
60
80
Voltage (mV)

Suppl Fig 2

A

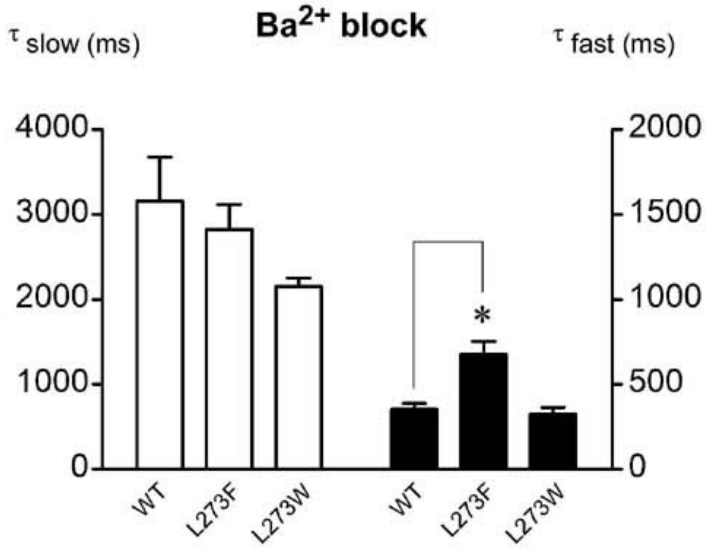

B

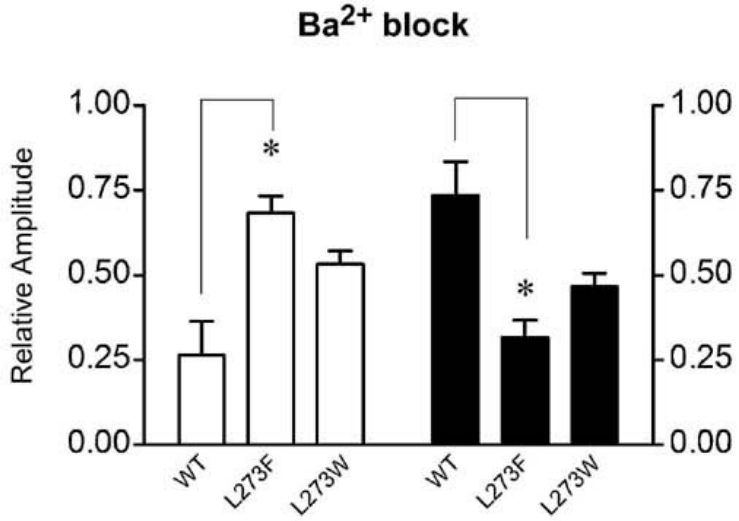

Suppl Fig 3

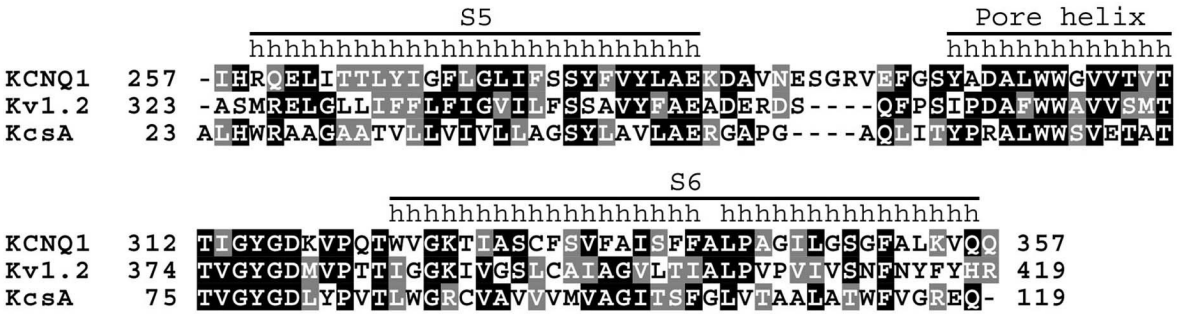
S5
Pore helix
hhhhhhhhhhhhhhhhhhhhhhhhhh
hhhhhhhhhhhhh
KCNQ1 257 -IHRQELITTLYIGFLGLIFSSYFVYLAEKDAVNESGRVEFGSYADALWWGVVTVT
Kv1.2 323 -ASMRELGLLIFFLFIGVILFSSAVYFAEADERDS----QFPSIPDAFWWAVVSMT
KcsA 23 ALHWRAAGAATVLLVIVLLAGSYLAVLAERGAPG----AQLITYPRALWWSVETAT
S6
hhhhhhhhhhhhhhhhhh hhhhhhhhhhhhhhh
KCNQ1 312 TIGYGDKVPQTWVGKTIASCFSVFAISFFALPAGILGSGFALKVQQ 357
Kv1.2 374 TVGYGDMVPTTIGGKIVGSLCAIAGVLTIALPVPVIVSNFNYFYHR 419
KcsA 75 TVGYGDLYPVTLWGRCVAVVVMVAGITSFGLVTAALATWFVGREQ- 119

Suppl Fig 4

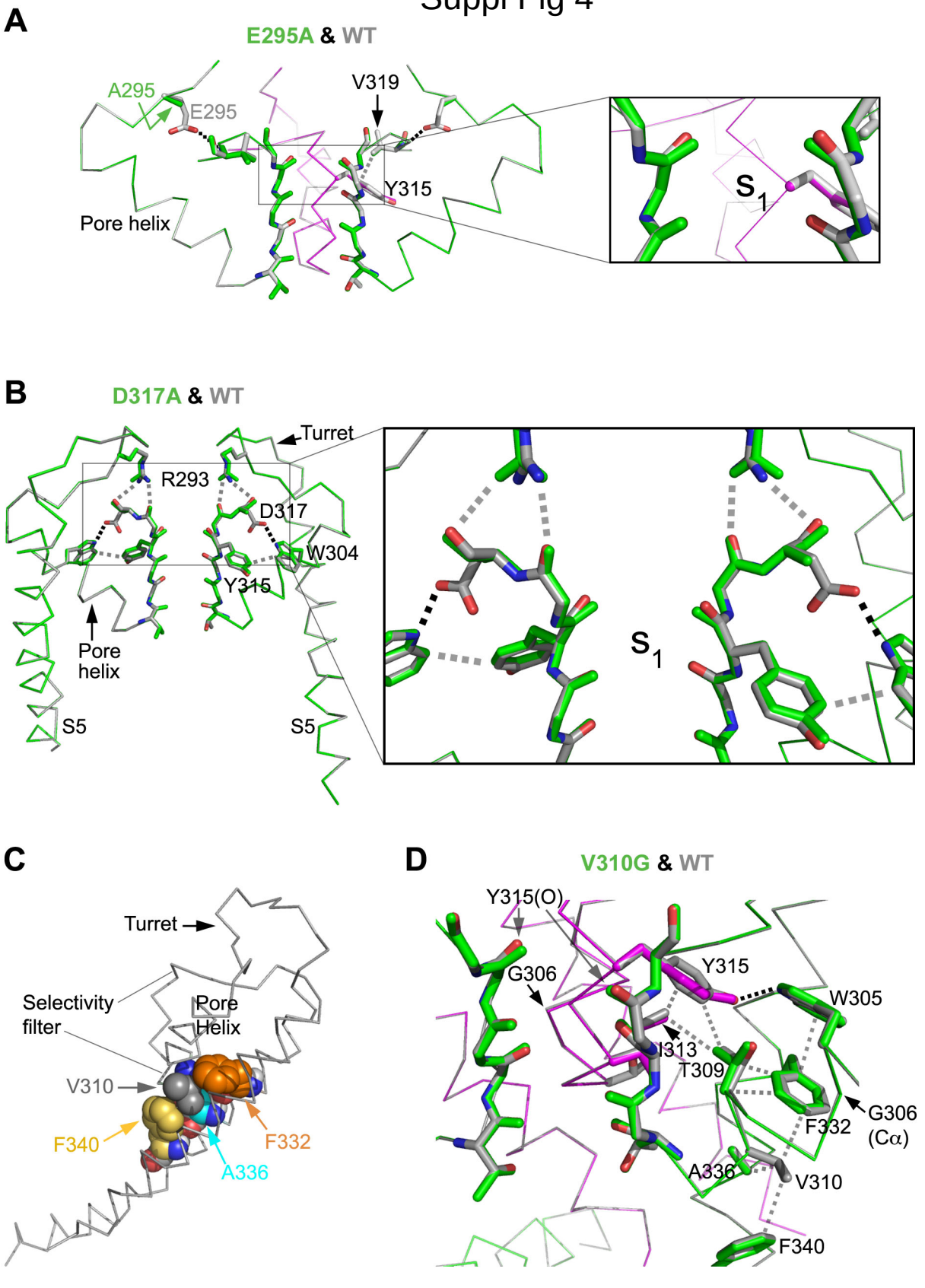
A
E295A & WT
A295
E295
V319
Y315
Pore helix
S1
B
D317A & WT
Turret
R293
D317
W304
Y315
Pore helix
S5
S5
S1
C
Turret
Selectivity filter
Pore Helix
V310
F340
F332
A336
D
V310G & WT
Y315(O)
G306
Y315
W305
I313
T309
F332
G306 (Cα)
A336
V310
F340

Suppl Fig 5

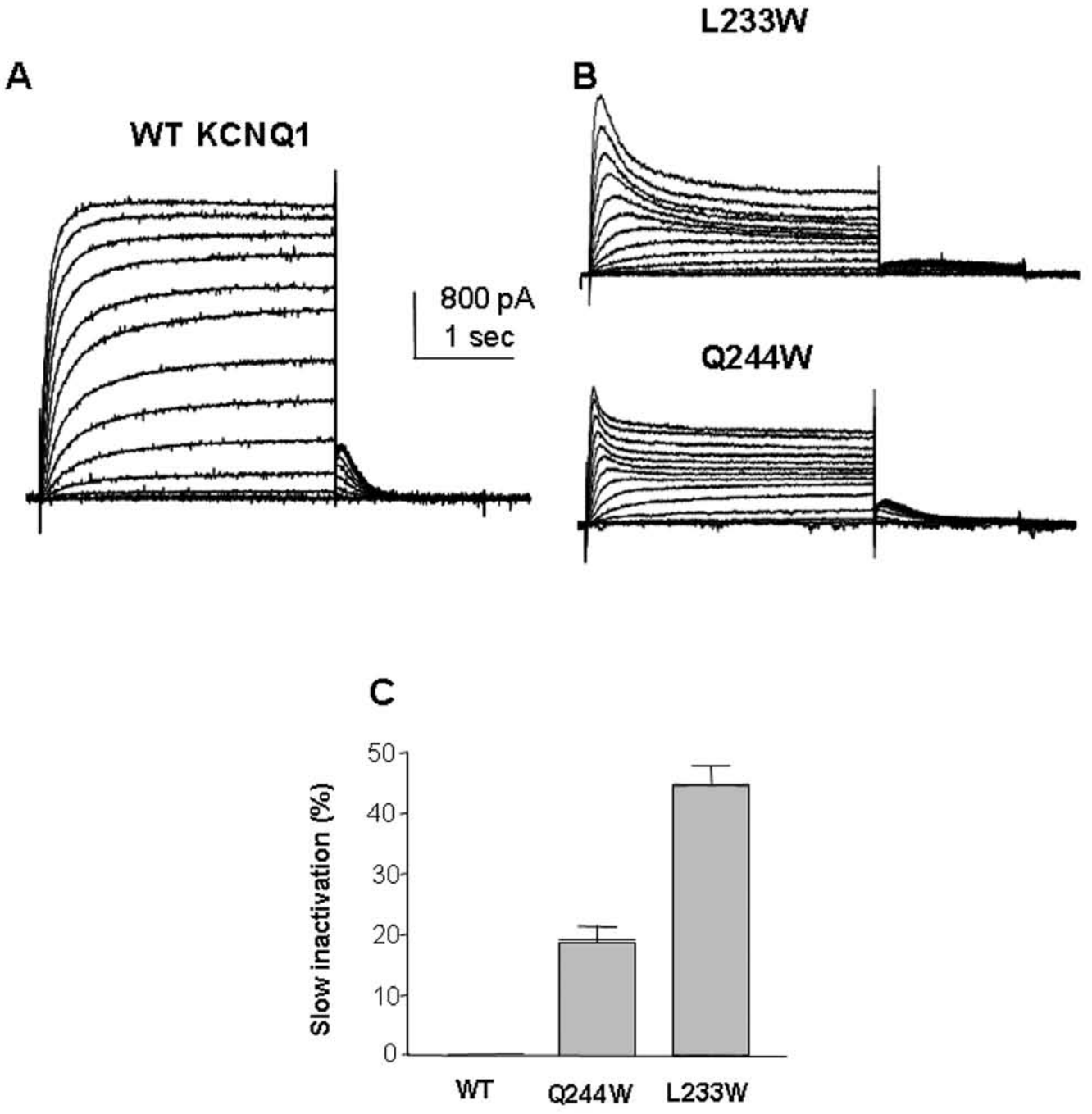
A
WT KCNQ1
800 pA
1 sec
B
L233W
Q244W
C
Slow inactivation (%)
50
40
30
20
10
0
WT
Q244W
L233W